International Journal of Pharmaceutics 683 (2025) 125993

Contents lists available at ScienceDirect

International Journal of Pharmaceutics

journal homepage: www.elsevier.com/locate/ijpharm

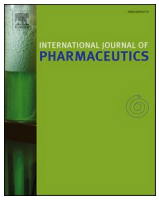

Hierarchical paclitaxel encapsulation in microbead-embedded microparticles for sustained ovarian cancer therapy☆

Cristina Chirizzi [a,1,2], Francesca Gorini [b,2], Ilaria Porello [a,2], Marco Malferrari [c], Maila Becconi [c], Elisa D'Arrigo [c], Francesco Falciani [c], Emma Coschina [b], Stefania Rapino [c,d], Anna Myriam Perrone [e,f], Pierandrea De Iaco [e,f], Pierangelo Metrangolo [a], Francesca Baldelli Bombelli [a], Gloria Ravegnini [b,g], Francesco Cellesi [a,*]

[a] Department of Chemistry, Materials, and Chemical Engineering "Giulio Natta", Politecnico di Milano, Via L. Mancinelli 7, 20131 Milan, Italy
[b] Department of Pharmacy and Biotechnology (FABIT), University of Bologna, Bologna 40126, Italy
[c] Department of Chemistry "Giacomo Ciamician", University of Bologna, Via Piero Gobetti 85, 40129 Bologna, Italy
[d] IRCCS Azienda Ospedaliero-Universitaria di Bologna 40138 Bologna, Italy
[e] Department of Medical and Surgical Sciences, University of Bologna, Bologna, Italy
[f] Division of Oncologic Gynecology, IRCCS Azienda Ospedaliero-Universitaria Di Bologna, Bologna, Italy
[g] Clinical Pharmacology Unit, IRCCS Azienda Ospedaliero-Universitaria di Bologna - Policlinico di Sant'Orsola, Italy

ARTICLE INFO

Keywords:
Ovarian cancer
Intraperitoneal chemotherapy
PLGA microparticles
Alginate microbeads
3D bioprinted tumor model

ABSTRACT

Ovarian cancer (OC) is the most lethal gynecologic malignancy, often diagnosed at advanced stages due to clinically silent peritoneal carcinomatosis. Although intraperitoneal (IP) chemotherapy enhances drug exposure, its effectiveness is hindered by rapid clearance, toxicity, and uneven distribution. To address these challenges, we developed a novel drug delivery system integrating paclitaxel (PTX)-loaded poly(lactic-co-glycolic acid) microparticles (PLGA-MPs) within calcium-alginate microbeads (Alg-MBs). This system aims to provide sustained drug release while minimizing adverse effects. PTX-loaded PLGA-MPs were prepared via solvent evaporation and encapsulated in Alg-MBs using a coaxial air jet generator. *In vitro* studies showed an initial burst release over five days, followed by sustained release until day 21, confirming the role of Alg-MBs in modulating drug diffusion. Cytotoxicity tests in 2D SKOV-3 OC cultures revealed dose-dependent effects, with increased PTX concentrations reducing cell viability. A 3D bioprinted tumor model was used to better replicate *in vivo* conditions and evaluate long-term efficacy. Sustained PTX release resulted in progressive tumor cell death over 21 days, with delayed but potent cytotoxicity at higher doses. These findings support hierarchical PTX microencapsulation for prolonged IP chemotherapy, while the 3D bioprinted model provided a more physiologically relevant platform for evaluating long-term therapeutic efficacy in OC treatment.

1. Introduction

Ovarian cancer (OC) is the most lethal cancer among the female cancers with nearly 250 000 women diagnosed each year and 140 000 deaths worldwide (Wojtyła et al., 2023). About 85% to 90% of malignant OCs are epithelial ovarian carcinomas, which are usually diagnosed in an advanced stage due to the presence of clinically silent peritoneal carcinomatosis. This devastating form of cancer progression is characterized by macroscopic tumor nodules within the abdominopelvic cavity, which develop because of peritoneal fluid circulation of spreading malignant cells (Fagotti et al., 2010; Pannu et al., 2003). Intraperitoneal (IP) chemotherapy has been developed to expose tumors in the peritoneal cavity to high drug concentrations; it has been safely administered to cancer patients and provides 20- to 1000-fold higher IP drug concentration than in plasma. Several clinical studies have demonstrated the activity of IP paclitaxel (PTX) and cisplatin (CPT)

☆ This article is part of a special issue entitled: 'Parenteral Time-Controlled Drug Delivery' published in International Journal of Pharmaceutics.

* Corresponding author.
E-mail address: francesco.cellesi@polimi.it (F. Cellesi).

[1] Current address: Neuroradiology Unit, Fondazione IRCCS Neurologico Carlo Besta, Milano 20100, Italy.
[2] Equally contributed.

https://doi.org/10.1016/j.ijpharm.2025.125993
Received 6 June 2025; Received in revised form 19 July 2025; Accepted 21 July 2025
Available online 26 July 2025

against advanced OC (Tsai et al., 2007). IP therapy yielded, on average, a 22% decrease in the risk of death and 12-month longer overall survival time, which is considered the most significant advance in OC research in the last decades (Tsai et al., 2007). Despite these advantages, the use of IP chemotherapy is limited by several complications, including infection due to prolonged use of indwelling catheter and local (intestinal) toxicity. These issues have prevented nearly 60% of patients from completing scheduled treatment cycles, leading to reluctance within the medical community to adopt IP therapy (Tsai et al., 2007). The pharmacological limitations of poor drug distribution and penetration within the abdominal cavity can be overcome through the Pressurized Intraperitoneal Aerosol Chemotherapy (PIPAC) or Hyperthermic Intraperitoneal Chemotherapy (HIPEC), which are relatively new techniques to deliver pressurized drug solutions into the abdomen (Graham et al., 2024; Leebmann and Piso, 2018; Tempfer et al., 2018). Nevertheless, IP delivery from single-dose applications is hindered by very rapid drug clearance (Tempfer et al., 2018). One approach to overcome IP therapy drawbacks is to use sustained drug release formulations that require less frequent dosing (Perelló-Trias et al., 2024; Primavera et al., 2021). Early research efforts in this area have shown promising results, particularly with biodegradable polymer microparticles (MPs) loaded with either PTX, CPT, or carboplatin (Cymbaluk-Płoska et al., 2019; Dwivedi et al., 2019; Kohane et al., 2006; Liu et al., 2023; Natsugoe et al., 1999; Tsai et al., 2013). Although poly(lactic-co-glycolic acid) (PLGA) is widely used as a polymeric biomaterial for drug delivery due to its excellent biocompatibility and biodegradability, PLGA-based microparticles (MPs) did not demonstrate promising results for intraperitoneal (IP) delivery in terms of minimizing adhesion formation. (Armstrong et al., 2006). *In vivo* tests highlighted a high incidence of polymeric residue and adhesions two weeks after injection, while histology revealed chronic inflammation, with prominence of foreign body giant cells (Kohane et al., 2006). Nanoparticles, or MPs made with low molecular weight PLGA appeared safer, but they are not suitable for sustained IP drug delivery, as they are cleared within two days (Kohane et al., 2006).

In the field of microencapsulation, hydrogel microbeads (MBs) have been widely used for IP delivery of therapeutic agents expressed by entrapped living cells (Calafiore and Basta, 2014; Qi et al., 2011). The hydrogel is a semipermeable material which allows diffusion while protecting the payload from immune response and unwanted cell/tissue interactions. Clinical trials demonstrated that after IP injection of human pancreatic islets encapsulated in calcium alginate (Ca-Alg) gels, insulin independence can persist for up to 9 months in type 1 diabetic patients (Ashimova et al., 2019). Alginate (Alg) is an anionic polysaccharide, which is considered the gold-standard material for cell microencapsulation, due to its high biocompatibility and high porosity of its gel (almost 98% wt. is water) (Lopez-Mendez et al., 2021). Ca-Alg MBs can be easily obtained by generating microdroplets from sodium alginate solutions, which are dropped into a Ca^{2+}-containing bath to achieve an almost instantaneous ionotropic gelation (Cellesi et al., 2004). Although Ca-Alg MPs implanted intraperitoneally may remain free and unattached to host tissues for months (Ashimova et al., 2019), they present large pores, which are good for cell encapsulation, but not for chemotherapeutic drug encapsulation, since release would be too fast for IP therapy (He et al., 2020).

Recent advances have led to the development of various composites consisting of nano- and MPs embedded in Ca-Alg microbeads or microcapsules (Hariyadi and Islam, 2020). These include the microencapsulation of PLGA (Win et al., 2024; Wu et al., 2013; Zhai et al., 2015), polystyrene (Kang et al., 2019), organogels (Sagiri et al., 2014) in alginate, with applications in drug delivery and diagnostics.

Therefore, the development of innovative methods for prolonged IP delivery of chemotherapeutic agents remains an unmet clinical need. In this context, a combination of the advantages of polymer MPs with gel MBs for the development of tailored drug delivery systems may represent a game-changer for the treatment of OC.

Based on this rationale, the aim of this study was to design and develop drug-loaded polyester MPs embedded within fully biocompatible, non-adhesive, and highly porous Ca-Alg MBs, enabling the sustained release of the chemotherapeutic agent (Fig. 1).

To achieve this goal, PTX was first encapsulated in PLGA microparticles (PLGA-MPs) using an oil-in-water (O/W) emulsion method. PLGA was selected as the polymeric material due to its excellent biocompatibility and biodegradability. The resulting microparticles were then incorporated into Ca-Alg microbeads (Alg-MBs) using a coaxial liquid–air flow nozzle, enabling the formation of a suspension of spherical particles with controlled physicochemical properties and sustained drug release over several weeks.

The efficacy of this delivery system was assessed and optimized through *in vitro* studies conducted on both two-dimensional (2D) and three-dimensional (3D) OC models. These experiments were designed in accordance with the 3Rs principles (Replacement, Reduction, and Refinement), aiming to minimize unnecessary animal testing and support the translation of biomaterials into advanced drug delivery systems for OC treatment. In particular, with reference to the Replacement principle, 3D cell cultures are among the most widely adopted experimental strategies to overcome the limitations of traditional 2D cultures, as they more accurately replicate key features of the extracellular matrix and cellular microenvironment, both of which significantly influence cell physiology (Quail and Joyce, 2013; Rodrigues et al., 2021). In this study, 3D OC models were fabricated using 3D bioprinting, a technology that has already demonstrated significant potential for creating 3D cellular models of various cancer types for drug development (Neufeld et al., 2022).

2. Materials and methods

2.1. Materials

Alginic acid sodium salt (viscosity 15–25 cps); Calcium chloride ($CaCl_2$, anhydrous, ≥ 93 %); Poly-vinyl alcohol (PVA, 80 % hydrolyzed, Mw = 9.000 – 10.000 Da); Polysorbate 80 (Tween 80); Poly(D,L-lactide-co-glycolide acid) (ester-terminated PLGA, 50/50) (Mw = 38,000 – 54,000 Da, RESOMER RG 504), Poly(DL-Lactide-co-glycolide)-Rhodamine B (Rhodamine B-grafted PLGA, 50/50, MW = 10000–30000 Da, Sigma-Aldrich.); Acetonitrile (ACN, 99.8 %); Dichloromethane (DCM, ≥ 99.9 %); Dimethyl sulfoxide (DMSO, ≥ 99.7 %); Sodium azide (NaN_3, 99 %); were all purchased from Sigma-Aldrich (Merck, Italy). Paclitaxel (PTX, Mw = 853.92 Da, 99.5 %); Poly(D,L-lactide-co-glycolide acid) 50/50, carboxylic acid-terminated (COOH-terminated PLGA) (Mw = 15,000 – 24,000 Da, abcr GmbH); were purchased from abcr GmbH (Karlsruhe, Germany).

Deionized water was obtained from Millipore Milli-Q purification unit (Type 1 Ultrapure Water, Merck Millipore).

2.2. PLGA MPs preparation and characterization

PTX-loaded PLGA MPs (PTX-MPs) were produced through an oil-in-water (O/W) single emulsion, based on a previously described method (Tsai et al., 2013). Four different PLGA formulations were tested, depending on the ratio between COOH-terminated PLGA and ester-terminated PLGA (100:0, 50:50, 25:75, 0:100 wt:wt, respectively).

38 mg of PLGA and 2 mg of PTX were separately dissolved in 0.5 mL of DCM each. After complete dissolution, the PLGA solution was transferred into the PTX solution and mixed for 15 min. Simultaneously, 4 mL of a PVA solution (1 % w/v) was withdrawn into a round-bottom flask and stirred at 200 RPM, fixing the temperature at 25°C. The resulting PLGA-PTX solution was then added dropwise to the PVA solution using a Pasteur pipette. This mixture was left under continuous stirring for 60 min. Subsequently, DCM was evaporated by means of a rotary evaporator. The initial pressure was set to 850 mbar and it was progressively decreased every 5 min until 400 mbar. The system was held at 400 mbar for 45 min to ensure complete DCM evaporation. The complete removal

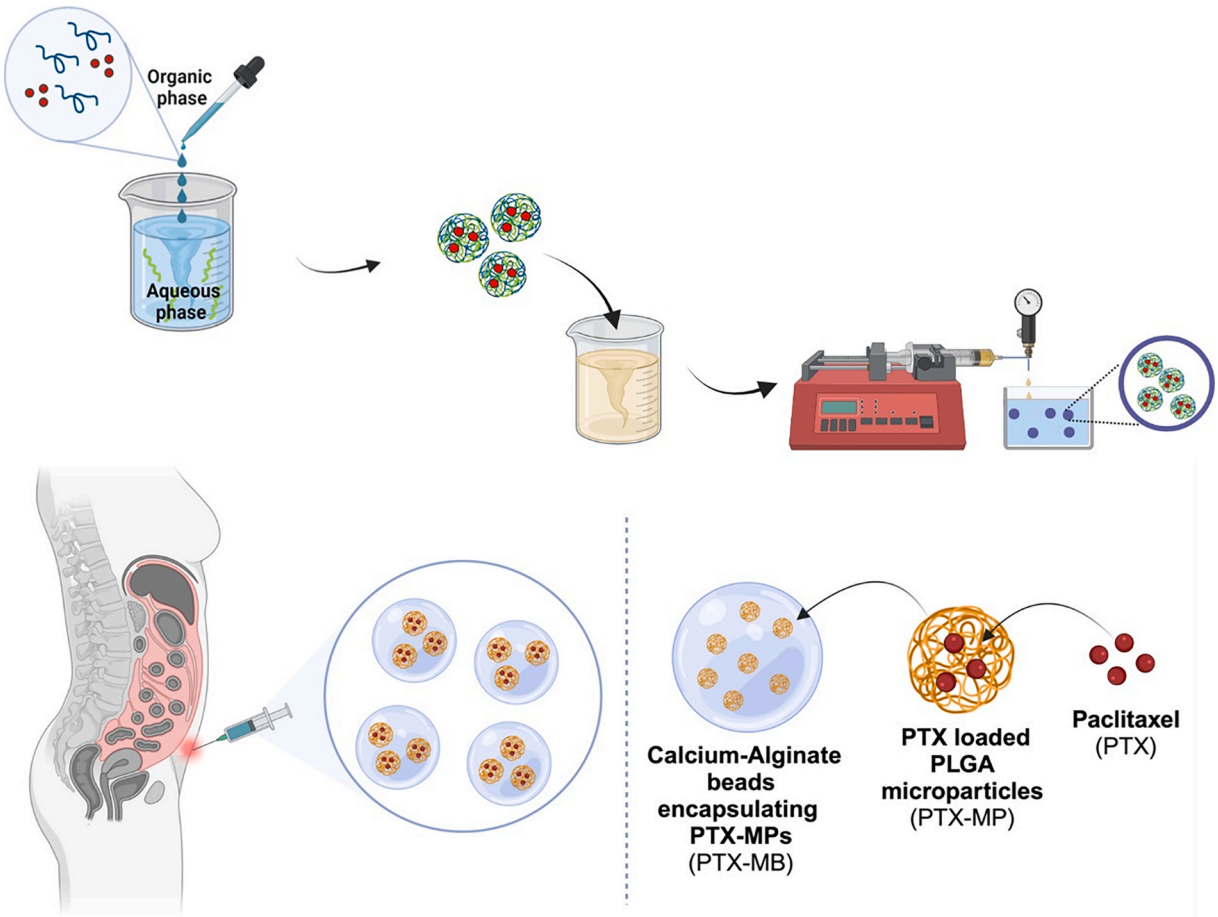

Fig. 1. Multistep preparation of PTX-loaded PLGA MPs embedded in Ca-Alg beads (PTX-MBs), as advanced drug delivery system for OC treatment.

of the organic solvent, aimed at minimizing potential cytotoxicity, was confirmed by NMR analysis (data not shown).

The resulting suspension was repeatedly washed with ultrapure water to remove unencapsulated PTX, residual surfactant, and other by-products. The purification was carried out via centrifugation at 5500 RPM for 1 min. The supernatant was removed with a Pasteur pipette, and the pellet was washed three times with 2 mL of Milli-Q water per wash. Following the washing steps, the particles were resuspended in 1 mL of Milli-Q water and stored in a refrigerator or freeze-dried to isolate the solid microparticles.

For the preparation of fluorescent MPs used in optical analysis, Rhodamine B-grafted PLGA was incorporated into the formulation at 2% w/w relative to the unlabeled PLGA. PLGA-MPs average diameters and particles size distribution were determined via optical microscopy analysis. 0.1 mL of purified PLGA-MPs suspension were dropped on a glass slide, covered with a coverslip and observed using an Olympus CH30 binocular optical microscope, equipped with an Olympus U-CMAD3 camera adapter and a set of three Olympus LMPlanFI lens objectives for magnification degrees of 5X, 10X, and 20X. Optical images were captured in real-time through Linksys32 software and processed with ImageJ software. MPs morphological characterization was performed by means of Scanning Electron Microscopy (SEM). A drop of MPs suspension was deposited using a Pasteur pipette on a piece of carbon conductive tape mounted on an aluminum stub, air dried at room temperature (r.t.) overnight, sputter coated with pure gold (S150B Edwards) and observed under an extended pressure SEM EVO 50 EP (Zeiss). Observations were performed in high vacuum conditions at 15 kV.

2.3. PTX loading quantification

0.2 mL of PTX-MP suspension were lyophilized using a Modulyo EF4-1596 freeze-dryer (Edwards). Subsequently, 0.2 mL of DMSO were added to dissolve PLGA and release the encapsulated PTX for quantification. PTX concentration was determined using an HPLC system (Jasco) equipped with a Restek C18 column and a photodiode array PDA detector. Detector wavelength was set at 270 nm, the mobile phase was composed of acetonitrile and water (52/48 v/v) in isocratic condition at a flow rate of 1 ml/min at 25°C. The concentration of PTX was quantitatively determined by comparison with a calibration curve based on drug concentrations ranging from 0.01 to 1 mg/mL. The encapsulation efficiency (EE) and drug loading (DL) were calculated as follows:

$$EE = \frac{mass\ of\ encapsulated\ PTX\ [mg]}{total\ mass\ of\ PTX\ used\ [mg]} \quad (1)$$

$$DL = \frac{mass\ of\ encapsulated\ PTX\ [mg]}{mass\ of\ solid\ phase\ [mg]} \quad (2)$$

Data were presented as mean ± standard deviation of three different replicates.

2.4. Ca-alginate microbeads preparation

3 ml of a 2.15 % w/v sodium alginate solution were mixed with 200 μL of PLGA-MPs suspension (either PTX-loaded or unloaded, 35 mg/mL) at r.t. for 5 min under magnetic stirring at 800 RPM, to achieve a final alginate concentration of 2% w/v. Alginate beads were obtained using an extrusion-dripping system composed of a 3 mL syringe (Norm-Ject)

filled with the Na-Alg suspension and securely locked to an Aladdin SyringeONE AL-1000 programmable single-channel infusion/withdrawal syringe pump. The syringe pump extruded the alginate suspension at a flow rate of 0.25 mL/min through a Nisco VARJ1 coaxial air flow nozzle (bead generator) (Nisco Engineering), which was connected to a compressed air tube at a flow rate of 12 L/min and at a pressure of 10 bar. The stainless still needle used for droplet formation and dripping had an inner diameter of 0.15mm and an outer diameter of 0.30 mm. After collecting the Na-Alg/PLGA-MPs mixture with the syringe, the air bubbles were removed by gravity and 2.2 mL of mixture were extruded into 6 mL of 0.1 M $CaCl_2$ bath, placed 12 cm above the dropping nozzle and maintained under stirring at 500 RPM. Ca-Alg microbeads (PTX-MBs) were formed as soon as the drops came in contact with $CaCl_2$ solution. Once the extrusion process was completed, MBs were left in the $CaCl_2$ bath for 20 min to obtain a gel with appropriate mechanical properties (Liu and Krishnan, 1999). The beads were purified via filtration through filter paper and washing them with Milli-Q water.

The same procedure was carried out to formulate empty Ca-Alginate beads (Alg-MBs), replacing PLGA MPs suspension with 200 μL of Milli-Q water.

Ca-alginate beads' size distribution curve was determined via optical microscopy analysis. 0.1 mL of beads suspension were dropped on a glass slide, covered with a coverslip and observed using an Olympus CH30 binocular optical microscope, equipped with an Olympus U-CMAD3 camera adapter and a set of three Olympus LMPlanFI lens objectives for magnification degrees of 5X, 10X, and 20X. Optical images were captured in real-time through Linksys32 software and processed with ImageJ software.

2.5. PTX release study from PTX-loaded microparticles and microbeads

In order to determine the cumulative PTX release profile diffusing from free PLGA-MPs or Alg-MBs, a release study simulating *in vitro* condition over 21 days was carried out. For the preparation of each sample, either 0.2 mL of PTX-loaded MPs suspension were immersed into 0.8 mL of buffer solution, or 0.7 g of Ca-Alg beads encapsulating PTX-PLGA MPs were immersed into 1.3 mL of buffer solution, to obtain a 2 mL sample for the test. The buffer solution was composed of PBS (10 mM, pH 7.4), Tween 80 (0.1 % w/v) and NaN_3 (0.02 % w/v). The Eppendorf tubes containing each sample were placed in a Thermo-Shaker TS-100 at 37 °C and maintained at a constant rotation speed of 300 RPM. At selected time points from day 1 to day 21, the samples were destructively analyzed withdrawing the entire supernatant and separating it from the pellet. The collected supernatants were freeze-dried and subsequently dissolved in 0.2 mL of DMSO for analysis. The amount of PTX released at each time point was evaluated using the same HPLC system at the same condition described for PTX loading evaluation. The cumulative PTX release was then calculated as the ration of PTX released at each time point and the initial amount of drug encapsulated into the beads. For statistical reasons, the procedure was carried out in triplicate for each time-point analyzed.

2.6. OC cell model

SKOV-3 cell line (HTB-77) was purchased from the American Type Culture Collection (ATCC). SKOV-3 were cultured in IMDM supplemented with 10,000 units/l of penicillin and streptomycin, 250 μg/ml amphotericin b, and 10 % (v/v) of sterile filtered (0.2 μm, cellulose acetate membrane) Fetal Bovine Serum (FBS) at 37 °C in a humidified atmosphere containing 5% CO_2. Media change was performed twice a week. Mycoplasma tests (MycoAlert Assay, Lonza Walkersville, Inc., USA) were performed regularly, on a 4-month basis.

The IC50 value for PTX (NSC 125973, Selleckchem) in the cellular model was evaluated by treating cells with increasing concentration of the drug. PTX powder was dissolved in DMSO to prepare the 10 mM stock solution, from which serial dilutions were subsequently prepared. 72 h after treatment, viability was assessed through CellTiter-Glo® (CTG) Luminescent Cell Viability Assay (Promega), following the manufacturer's instructions. The IC50 value was calculated using GraphPad Prism version 10.0.0 for Windows, GraphPad Software, Boston, Massachusetts USA, https://www.graphpad.com.

2.7. In vitro evaluation of PTX-MPs efficacy

Firstly, the effect of PTX-MPs was evaluated: on day 0, 30 000 cells per well were seeded in a 24-well plate. At day 1, lyophilized PTX-MPs were resuspended in Milli-Q water and sterilized for 30 min under UV light; after that, serial dilutions of PTX-MPs in medium were prepared and cells were treated with different PTX concentrations. DMSO and free PTX at IC50 concentration were used as controls. The same volumes of PLGA-MPs were used to evaluate the potential cytotoxic effect of the water content on the cells. Cells were monitored for 7 days through the IncuCyte S3 (Sartorius), which determines label-free measurements of cell growth based on area (confluence) or cell number (count) metrics, both of which are generated via segmentation (masking) of high-quality phase images. Phase area confluence was automatically released by the instrument after setting-up the masking manually. Viability was assessed through the CTG assay, a homogeneous method to determine the number of viable cells in culture based on quantitation of the ATP present, which signals the presence of metabolically active cells. All the experiments were performed in duplicate.

2.8. In vitro evaluation of PTX-MBs efficacy

Subsequently, experiments with PTX-MBs were carried out; treatments were performed with both Alg-MBs and PTX–MBs. At day 0, 55 000 cells per well were seeded in a 12-well plate. On day 1, MBs were deprived of the $CaCl_2$ solution in which they were immersed and washed twice with Milli-Q water. Subsequently, Alg-MBs and PTX-MBs were resuspended in culture medium, and sterilized for 30 min under UV light. Then, cells were treated with different volumes of MBs corresponding to different concentrations of PTX with Alg-MBs used to assess their toxicity on the cellular models. Viability was assessed after 7 days as previously described. All the experiments were performed in duplicate.

2.9. 3D bioprinted OC cell models and MP/MB assessment

3D bioprinted OC models were prepared by using a BIO X Bioprinter (Cellink, a BICO Company). Optimization of the bioink formulation was previously reported (Becconi et al., 2023; Pagnotta et al., 2023). SKOV-3 cells were harvested from bidimentional cell culture and resuspended in the alginate bioink at a final concentration of 4 x 10^6 cells per mL. 3D bioprinted OC constructs with 1 cm size were printed on 24-well plates and crosslinked for 5 min with 200 mM $CaCl_2$ just after printing. After extensive washing with phosphate buffered saline (PBS), constructs were immersed in a complete cell growing medium and maintained in the incubator (37°C, 5% CO_2).

Live-dead analysis with calcein-AM/propidium iodide (calcein-AM, ThermoFisher product no. C1430; propidium iodide, Merck product no. P4864) was performed as previously described (Cantelli et al., 2021). After washing with PBS, 3D bioprinted OC models were incubated for 30 min with 4 μM calcein-AM and 4 μM propidium iodide in HBSS (Hanks Balanced Salt Solution medium, Merck product no. H8264) under culturing conditions (37°C, 5% CO_2). After washing with PBS, the constructs were covered with HBSS during data acquisition. Nikon Eclipse TiS inverted fluorescence microscope was employed for acquisition of wide field fluorescence images, by using Nikon Texas Red HYQ cubic filter (λ excitation = 532–587 nm, λ emission = 608–683 nm) for propidium iodide and a Nikon FITC cubic filter (λ excitation = 465–495 nm, λ emission = 515–555 nm) for calcein-AM.

Viability of the PTX-treated 3D models was assessed by adding PTX

in the culture medium at different concentrations (*i.e.* 15, 100 and 200 nM) the day after the printing process; media change was performed every 3–4 days adding fresh PTX. Viability was evaluated after 14 days by AlamarBlue™ Cell Viability Reagent (Invitrogen). Briefly, 10% of the reagent was added into the culture medium; the plate was incubated at 37°C for up to 3 hrs. Absorbance was then read in a Tecan plate reader at 570 nM (using 600 nM reference wavelength). To assess the efficacy of MPs and MBs on 3D bioprinted models, these materials were accurately resuspended in culture medium as previously described. The day after the printing process, the particles were added to culture medium and gently transferred to the 3D models which were incubated until the readouts, performed at 24 h, 48 h, 72 h, 7 days, 14 days and 21 days. Media change was performed every 3–4 days. In the case of PTX-MBs, considering the huge dimension of Alg-MBs media change was performed leaving MBs on the bottom of the well, to evaluate long-term release of the drug. Cell viability in 3D models was assessed using AlamarBlue™ Cell Viability Reagent (Invitrogen) as previously described.

To visually inspect viable cells within the 3D bioprinted construct, the ReadyProbes® Cell Viability Imaging Kit (Blue/Green) (Invitrogen, R37609) was used. Confocal fluorescence images were acquired with a Nikon A1R confocal microscope, using two laser lines (401 and 489 nm) and two detection channels (460/30 nm and 525/50 nm) for the NuncBlue and NuncGreen dyes respectively. For these analyses, after bioprinting, the 3D OC constructs were cultured for 7 days and then treated for 72 h with PTX 15 nM dissolved in the growing medium or 1500 nM PTX-MPs. Before image acquisition, OC models were transferred to 3.5 cm diameter Petri dishes and incubated with ReadyProbe Kits for 5 min, as indicated by the producer; briefly, 2 drops of NucBlue® Live reagent (Hoechst 33342) and NucGreen® Dead reagent were added to 1 ml of cell growth media, then viability was determined by counting total vs dead cells through a confocal microscope. Confocal images were acquired just after this incubation.

3. Results and discussion

3.1. Preparation and characterization of PTX-MPs

PLGA microparticles were prepared following a solvent evaporation method (Tsai et al., 2013), where PTX and PLGA were mixed in DCM, emulsified in a PVA solution, and then the solvent was removed. The resulting particles were collected, washed, and either stored as a suspension or freeze-dried into powder.

Four different PLGA formulations were evaluated in terms of particle size, drug loading, and encapsulation efficiency to investigate the influence of the ratio between ester-terminated and COOH-terminated PLGA, as these two different terminal groups (lipo- and hydro-philic, respectively) may have different effects on particle formation, surface properties, and drug loading. Particle diameter remained relatively consistent across formulations, except for the 100% COOH-terminated PLGA, which exhibited the largest average size (5 μm) (Fig. S1a, Supporting Information, SI). In contrast, the impact of PLGA composition was more pronounced in PTX encapsulation efficiency. While drug loading remained around 5% across all formulations, encapsulation efficiency was highest for the 100% COOH-terminated PLGA (Fig. S1b, SI). This suggests a reduction in PTX loss during the encapsulation process, likely due to the lower formation of sub-micron particles, which are typically lost during the washing and centrifugation steps. According to these results, 100% COOH-terminated PLGA formulation was selected for the preparation of the PLGA-MPs.

Particle size and morphology were characterized by optical microscopy (OM) and scanning electron microscopy (SEM). According to OM and SEM images (Fig. 2), PLGA MPs were spherical in shape with a smooth surface without visible PTX crystals. Particle size distribution, which was obtained by the analysis of the average diameter of each particle in OM, shows an average particle size of 5 μm. The asymmetry in the particle size distribution can likely be attributed to the centrifugation step during purification, as particles smaller than 1 μm may remain suspended in the supernatant and consequently removed.

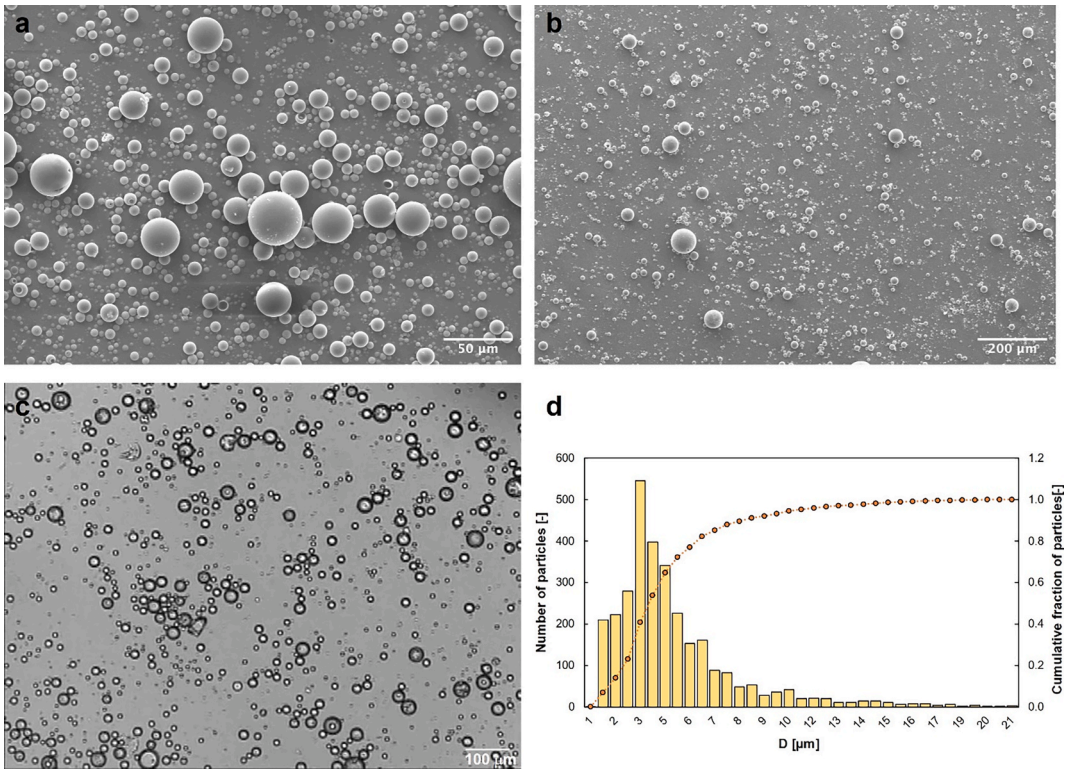

Fig. 2. a,b) SEM images of MPs at different magnification. c) OM image of MPs. d) Size distribution of PTX-MPs.

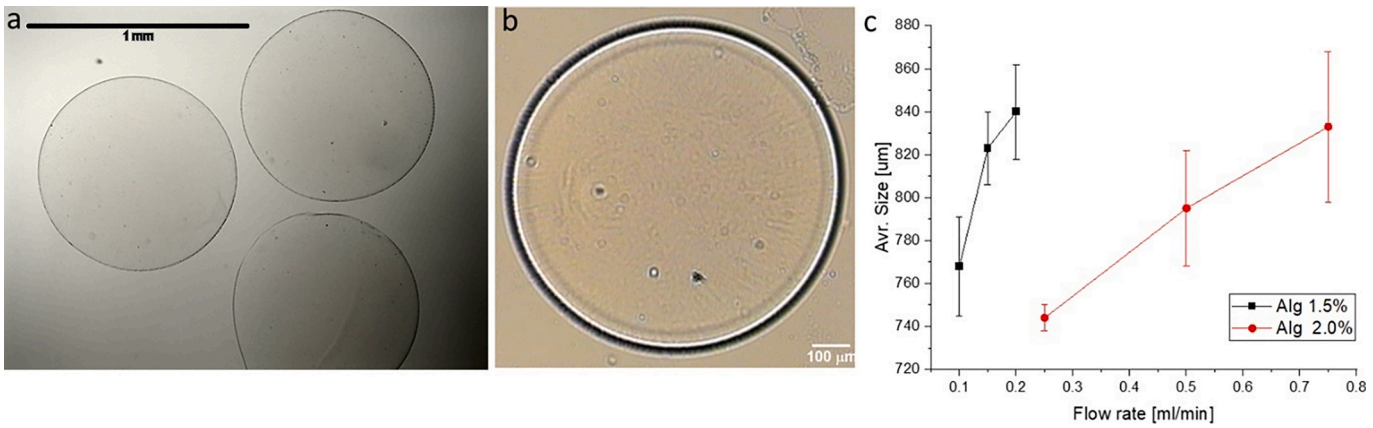

Fig. 3. a) OM image of Ca-Alg beads (scale bar 1 mm) obtained via coaxial bead generator. b) with a detailed view of a single spherical bead (scale bar 100 µm). c) Particle diameter (750–850 µm) can be tuned by varying the flow rate of the alginate solution and its concentration (between 1.5 and 2% wt.).

3.2. Preparation and characterization of alginate microbeads

Alginate beads were prepared using a coaxial (air jet) bead generator. In this system, gel MBs are formed by extruding a Na-alginate solution through a syringe fitted with an appropriately sized needle, using a piston pump. The coaxial air stream facilitates the formation of droplets by pulling them from the needle tip into a $CaCl_2$ gelling bath. This process produced spherical Ca-Alg gel beads with diameters that can be tuned based on the flow rate and alginate concentration of the extruded liquid phase (Fig. 3). A Na-alginate concentration of 2% was found to be optimal, resulting in gel beads with good stability and mechanical stiffness, in agreement with previous microencapsulation studies (de Jesus et al., 2019).

To encapsulate PLGA-MPs within alginate microbeads, a suspension of PLGA-MPs in water (either PTX-loaded or unloaded) was premixed with a Na-alginate solution to achieve a final alginate concentration of 2% w/v. The highest amount of PLGA-MPs successfully encapsulated was 35 mg per ml of gel. At higher PLGA concentrations, the laminar jet flow became too unstable during extrusion, preventing the formation of spherical and homogeneous microbeads.

Optical images of the resulting gel microbeads at different magnifications are shown in Fig. 4. In Fig. 4A, the presence and distribution of PLGA-MPs are highlighted by red staining, achieved by incorporating 2% w/w of Rhodamine B-grafted PLGA into the PLGA solid formulation prior to microparticle formation. No appreciable differences were observed when PTX-loaded MPs were encapsulated instead (Fig. 4B). The PLGA-MPs appeared randomly distributed within the Ca-Alg matrix without affecting the overall shape and morphology of the MBs.

The OM analysis provided a particle size distribution (Fig. 4C) with a diameter range of 600–760 µm, which is slightly smaller than that of the unloaded Alg-MBs (750–850 µm). This reduction in size, which is advantageous for increasing the surface area per unit gel volume, may be attributed to the influence of the PLGA-MPs suspension on the laminar jet flow and microdroplet formation during the extrusion process.

3.3. In vitro drug release

The *in vitro* release of PTX from MPs under physiological conditions was analyzed over a 21-day period. The release profiles, presented in Fig. 5, demonstrate that PTX-MPs exhibited a typical biphasic release pattern, with an initial burst phase during the first five days, followed by a more sustained release over approximately two weeks. Complete PTX release (~100 %) was achieved at around 20 days, consistent with the gradual erosion of the PLGA matrix throughout the study. When PLGA microparticles were encapsulated within Alg-MBs, the release plateau remained comparable to that of the free PLGA; however, a markedly slower and more sustained release was observed during the first 10 days. This suggests that the Ca-Alg gel matrix modulates PTX diffusion by restricting its transport through the porous network. Furthermore, OM analysis (Fig. 5b–c) provide evidence of PLGA microparticle degradation within the alginate gel, as indicated by the near-total disappearance of PLGA MP domains by day 21, correlating with the completion of PTX release.

3.4. In vitro assessment of the MP/MB system in 2D OC cell models

The biocompatibility and the efficacy of this delivery system was first evaluated *in vitro* using a 2D culture of SKOV-3 cells. To determine the cytotoxic potential of MP/MB system, we evaluated viability of SKOV-3 cells treated with different amounts/concentrations of MPs/MBs; treatment with free PTX was used as a positive control. An IC50 value of 15 nM for PTX was determined in this cell line after 72 h of incubation. SKOV-3 treated with PTX-MPs at PTX concentrations ranging from 15 nM to 150 nM (corresponding to 1xIC15 to 10xIC50) did not cause decrease in cell viability, similarly to what observed for PTX-free MPs. In contrast, treatment with PTX-MPs at 30xIC50 (450 nM), 50xIC50 (750 nM) and 100xIC50 (1500 nM) caused a significant decrease in cell viability and cell density (phase area confluence) (Fig. 6). Clearly, the delayed release of PTX from MPs sustains lower drug concentrations over time, which may lead to an altered pharmacodynamic response, and a shift in its toxic effect from the IC50. Moreover, the shift may also be influenced by differences in test conditions, such as the absence of organic solvents typically required to dissolve the drug (Arokia Femina et al., 2023; Larsson et al., 2020). Overall, while sustained PTX release may result in reduced immediate cytotoxicity, it offers potential therapeutic advantages, including decreased systemic toxicity, prolonged tumor exposure, improved drug distribution, and a reduced risk of resistance.

Once the lack of toxicity of the PLGA-MPs and the pharmacological effect of the PTX-MPs were confirmed, PTX-MBs effect was evaluated on the same cell line, at final PTX concentration of 100xIC50 (1500 nM) and 200xIC50 (3000 nM). Alg-MBs (PTX-free) at the same volume fraction corresponding to 20xIC50 and 200xIC50 were used as negative controls (Fig. S2, SI).

Results revealed a high mortality rate in cells treated with 100X and 200XIC50 values of PTX-MBs. However, an increase in mortality was also observed in cells treated with the highest concentration of Alg-MBs. This unexpected toxicity could be attributed to the relatively large volume occupied by Alg-MBs, which may hinder oxygen and nutrient exchange by covering the entire cell layer. For the same reason, the

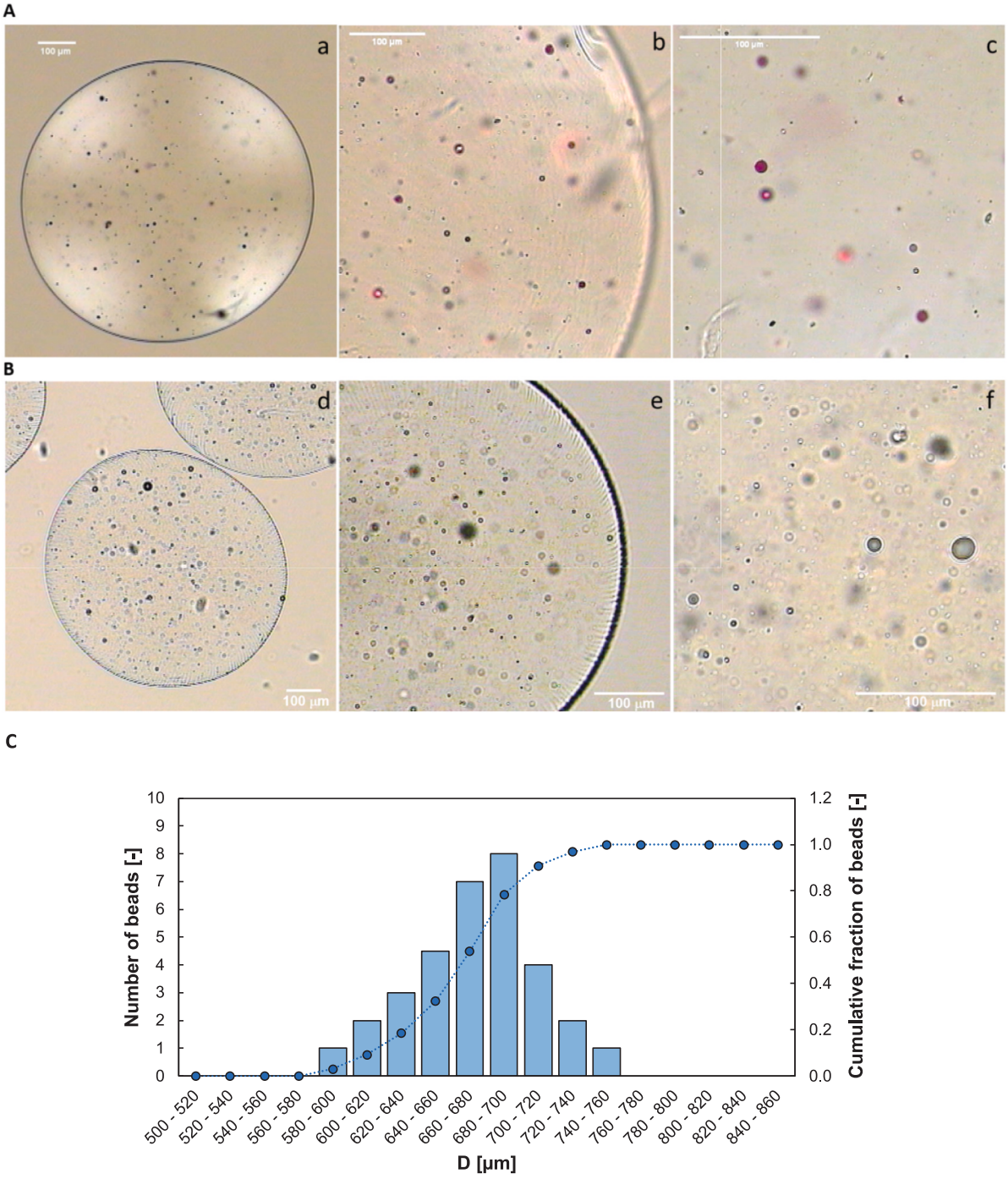

Fig. 4. A) OM images of Ca-Alg MBs loaded with PLGA MPs, at different magnification (5x (a), 10x (b), 20x (c)); PLGA was stained with grafted Rhodamine B. B) OM images of Ca-Alg MBs loaded with PTX-PLGA MPs (5x (d), 10x (e), 20x (f)). C) Particle size distribution of Ca-Alg MBs loaded with PTX-PLGA MPs, obtained by the OM analysis of the average bead diameter.

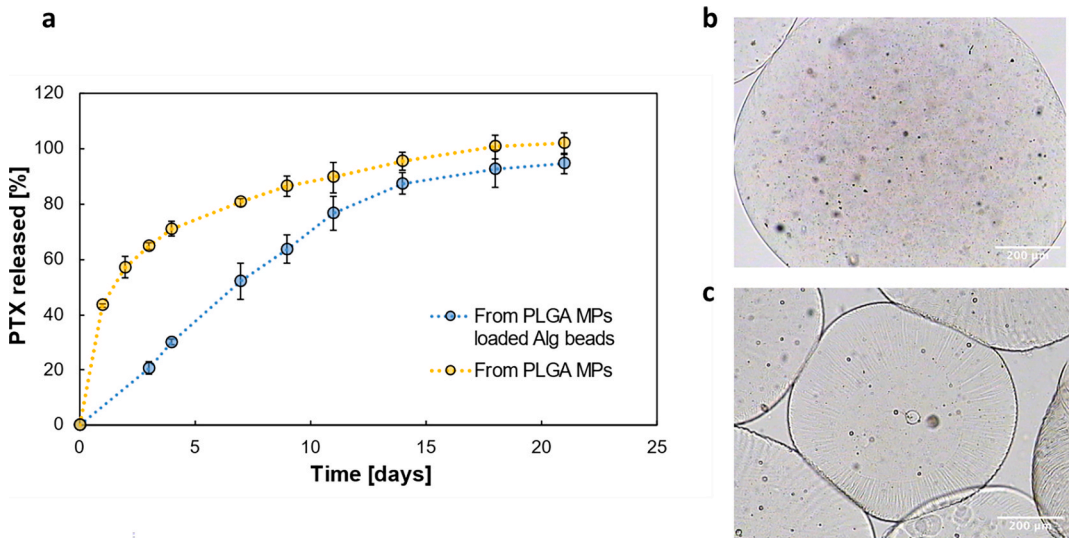

Fig. 5. a) Drug release-time profiles from PTX-PLGA MBs and PTX-PLGA-Alg MBs in PBS 10 mM, pH 7.4, at 37 °C, for 21 days. (b) OM image of the PTX-PLGA-Alg MBs at day 0 and (c) at day 21.

IncuCyte camera was also more difficult to focus, and the results were not as clear as those for MPs alone (Fig. S2b, SI). Moreover, the experiments could not be performed over 7 days due to the cells reaching confluence in the well. For this reasons, 3D bioprinted models were designed and exploited to better mimic the *in vivo* tumor mass.

3.5. *In vitro assessment of the MP/MB system in 3D bioprinted OC cell models*

It was crucial to perform tests on *in vitro* models that more accurately mimic the complexity of the *in vivo* tissue in order to assess the diffusion of the released drug within a three-dimensional (3D) tissue and to examine the cellular response within a 3D structure. Moreover, since the aim of the study was to evaluate the controlled release of this system and its subsequent long-term effect, 2D cell cultures did not constitute the optimal cell model, as experiments could only be conducted for a maximum duration of 3–7 days; the 3D cell culture can, instead, be continued for several weeks. For this reason, a 3D bioprinted model was employed for the SKOV-3 cell line and maintained in culture for up to 21 days. The bioink used for the OC 3D constructs was based on an alginate formulation previously established with other cancer cell models (Becconi et al., 2023). Both the extrusion bioprinting procedure and cell behavior in the 3D construct over extended culturing periods (approximately 4 weeks) were previously well-characterized. This included analysis of cell aggregate distribution over time, expression of cell–cell adhesion markers, and the assessment of key features of the cellular chemical microenvironment, such as oxygen gradients (Becconi et al., 2023). An optimized bioink formulation was employed in the present work to prepare 3D bioprinted cubic constructs as shown in Fig. 7a–c. SKOV-3 viability at 24 h, 48 h and 72 h post printing was assessed using calcein-AM/propidium iodide assay, as described in the *Materials and Methods* paragraph. The results (Fig. 7d) show high SKOV-3 cell viability, remaining approximately constant at 80% of the total cell population in the 3D bioprinted constructs.

PTX effect on viability of SKOV-3 bioprinted cells was investigated with Alamar blue assays (see *Materials and Methods* section for detailed description of the assay) upon 14 days of culturing with different dissolved PTX concentrations in the cell culturing medium of 15 nM, 100 nM, and 200 nM. The results (Fig. S3, SI) suggested that while approximately 50% of cell viability is retained up to 7 days of culturing with PTX 15 nM, low viability was clearly produced with PTX 100 and 200 nM already after 3 days that lead to complete death of the SKOV-3 cell population at 7 days of culturing. Complete killing of OC cells was observed at 14 days of culturing for PTX 15 nM.

Once the 3D bioprinted model was established, the pharmacological effect of MPs/MBs systems was evaluated. The time course of SKOV-3 viability upon incubation with PTX-MPs at different concentrations, corresponding to a total PTX concentration in the well equal to IC50 (15 nM), 30xIC50 (450 nM), 50xIC50 (750 nM) and 100xIC50 (1500 nM) was evaluated. The test was carried out over 21-day treatment of OC 3D bioprinted models, using free PTX at 15 nM (IC50) as a positive control. The results (Fig. 8) showed that efficient killing of the SKOV-3 cells embedded in the OC 3D bioprinted models at 21 days of culturing was demonstrated with PTX released from PTX-MPs at 750 nM and 1500 nM. Although differences in drug sensitivity between 2D and 3D culture systems may be expected (Muguruma et al., 2020), cell death comparable with that observed with 15 nM PTX in the cell culture medium was achieved under these experimental conditions. Continuous decrease of cell viability was clearly observed over the 21-day period of treatment for these PTX release doses, showing efficacious and persistent PTX effect on cancer cell viability from PTX-MPs. Interestingly, a continuous, slow decrease of cell survival was observed up to 21 days even at lower released concentrations of PTX from PTX-MPs (*i.e.*, 30 nM and 450 nM); these observations strongly support the employment of PTX-MPs for persistent and controlled release of drugs *in situ*, through modulation of drug loaded in the MPs. Higher concentrations are required to achieve the same drug sensitivity as free PTX, as the continuous delivery from the particles maintains a lower concentration over time. Additionally, periodic medium replacement, necessary to prevent nutrient depletion and maintain consistent experimental conditions over multiple days, further reduced overall drug exposure.

The results of the Alamar Blue assay on PTX-MPs treatment of 3D bioprinted OC model were confirmed by confocal analysis of OC cell population viability with ReadyProbes (see *Materials and Methods* section for more details), which employ NucBlue reagents to stain living cells and NucGreen reagents to stain dead cells. This analysis allows for a spatially resolved view of the effects of PTX release from PTX-MPs on the overall OC population in the 3D structure. Untreated OC models and OC models treated for 72 h with either PTX-MPs (1500 nM) or free PTX (15 nM) directly added to cell culture medium, were analyzed. Representative images of the live-dead staining are showed in Fig. 9a–c; the results of the live-dead analysis (Fig. 9d) are in good agreement with those obtained with the Alamar Blue assay and confirmed that efficient release of PTX can be obtained with appropriate loading of PTX on MPs and that the viability of the cells in the 3D structure is homogeneously affected.

The toxicity caused by Alg-MBs in 2D cell models was not observed in

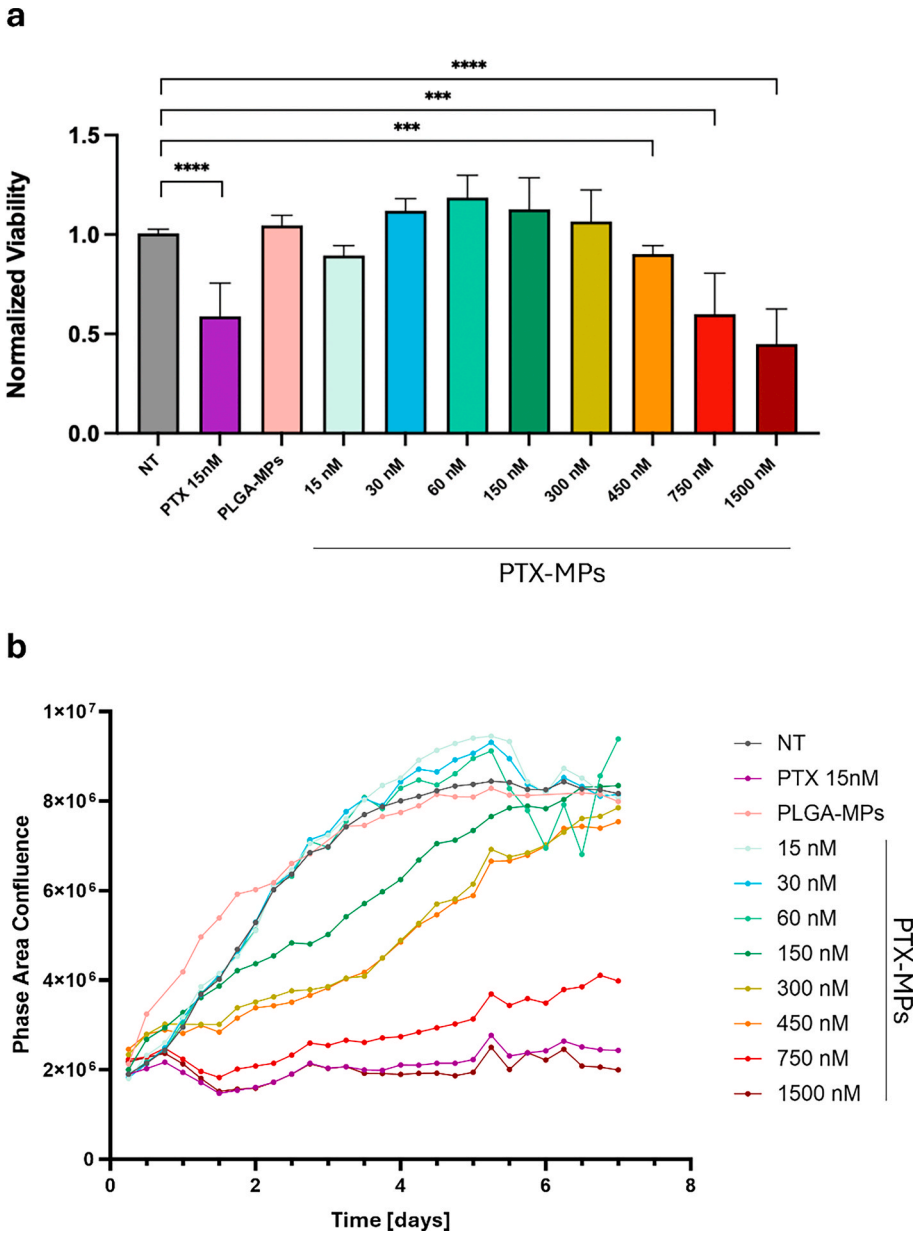

Fig. 6. Effect of PTX-MPs and PLGA-MPs on SKOV-3 model. a) Results obtained through the CTG assay after 7 days; b) Phase Area Confluence results obtained by IncuCyte S3 (Sartorius) over 7 days from seeding. Free PTX at the IC50 (IC50 PTX) concentration was used as positive control; ***$p < 0.001$, **** $p < 0.0001$. Cell viability values for treated groups were normalized to the no-treatment (NT) control, which consisted of cells cultured with DMSO (solvent used to resuspend PTX) and was assigned a value of 1 (100% viability). PLGA-MPs refer to PTX-free PLGA microparticles, used at a particle volume equivalent to that of the highest dose group (corresponding to 100 × IC50).

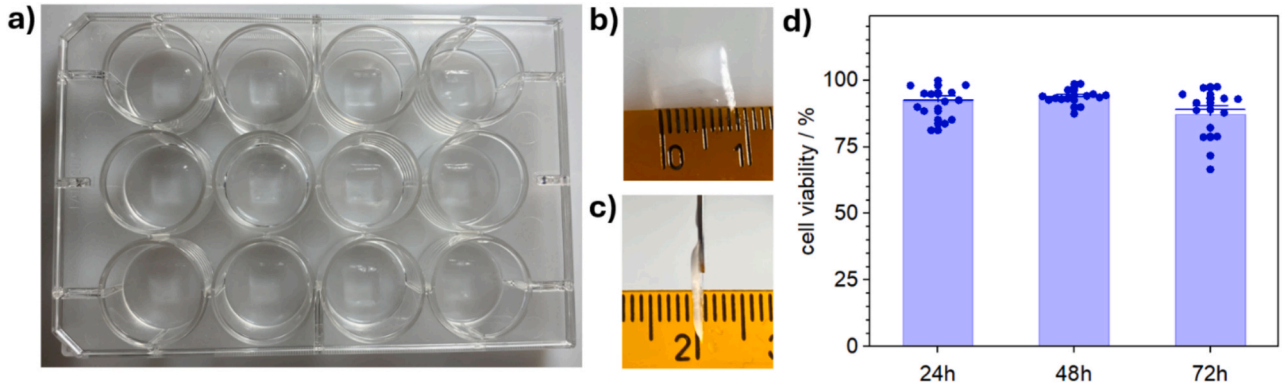

Fig. 7. 3D Bioprinted OC model and OC cell viability after bioprinting. Pictures of a representative set of OC bioprinted constructs (a-c) and percentage of cell viability (d) at 24 h, 48 h and 72 h after bioprinting. Cell viability was estimated with calcein-AM/propidium iodide; bars refer to the average, large lines to median and bar intervals to 1.5 standard errors.

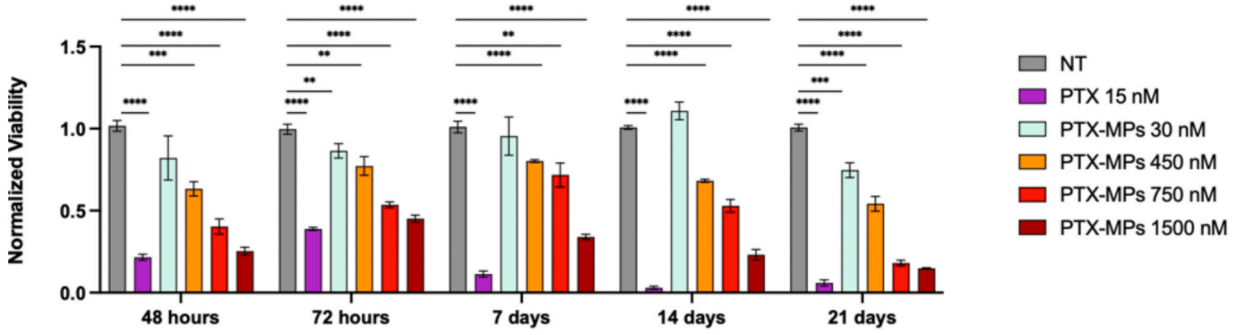

Fig. 8. Viability of SKOV-3 cells bioprinted in 3D models after treatment with PTX-MPs **: $p < 0.01$; ***: $p < 0.001$; ****: $p < 0.0001$. "NT" (no treatment) indicates cells grown with DMSO (solvent used to resuspend PTX). Cell viability values for treated groups were normalized to the NT control, which was assigned a value of 1 (100 % viability).

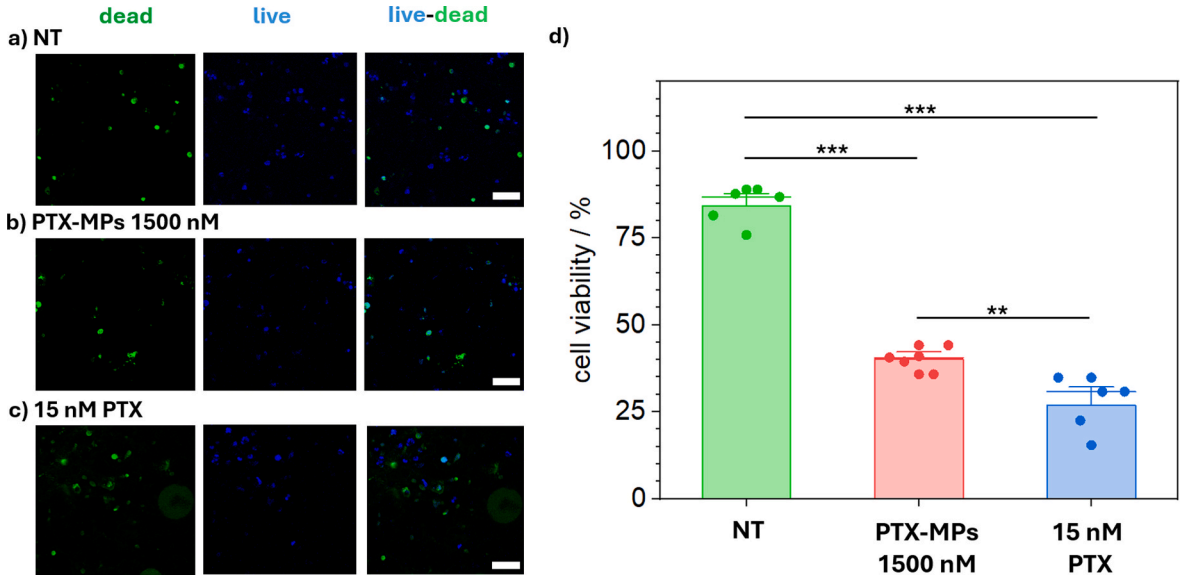

Fig. 9. Viability of 3D OC bioprinted models. Confocal microscopy images of live-dead analyses using NucBlue/NucGreen dyes (live, blue: excitation 401 nm, emission 460/30 nm; dead, green: excitation 489 nm, emission 525/50 nm; scale bar: 100 μm); a) control, not treated (NT) 3D constructs; b) following 72 h treatment with PTX-PMs 1500 nM; c) following 72 h treatment with PTX 15 nM. Confocal microscopy images of live-dead analyses and (d) percentage of cell viability, expressed as the number of cell viable divided by the total number of cells, two sample *t*-test **, $p < 0.01$; ***, $p < 0.001$. (For interpretation of the references to colour in this figure legend, the reader is referred to the web version of this article.)

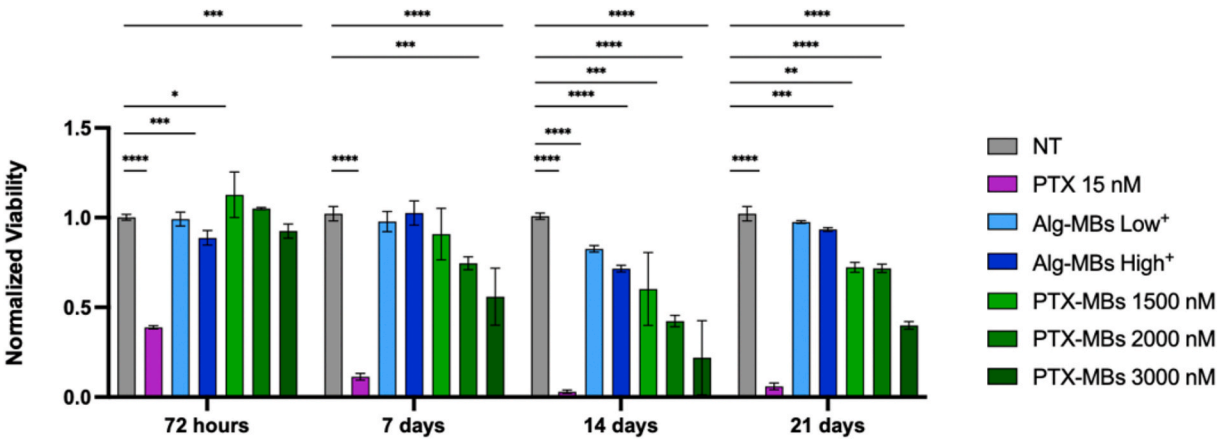

Fig. 10. Viability of SKOV-3 cells bioprinted in 3D models after treatment with Alg-MBs and PTX-MBs at different concentrations, using free PTX at 15 nM (IC50) as positive control; *: $p < 0.05$; **: $p < 0.01$; ***: $p < 0.001$; ****: $p < 0.0001$. + "Low" and "High" refer to the volumes of Alg-MBs used as controls in absence of drug, with "High" representing the maximum volume for the highest PTX concentration, and "Low" representing the minimum volume for the lowest PTX concentration. "NT" (no treatment) indicates cells treated grown DMSO (solvent used to resuspend PTX). Cell viability values for treated groups were normalized to the NT (no treatment) control, which was assigned a value of 1 (100 % viability).

3D models up to 21 days, even at the highest volumes of Alg-MBs used, as shown in Fig. 10. Moreover, Fig. 10 shows the pharmacological effect of PTX-MBs at the final PTX concentration of 1500 nM, 2000 nM, and 3000 nM. The effect of PTX-MBs was found to be delayed, showing no effects on viability at 72 h post treatment. However, a significant decrease in viability was observed at 7 days at the highest PTX-MPs concentration. Considering longer time points (*i.e.*, 14 and 21 days), the effect observed at the highest concentration is even more pronounced.

Therefore, MBs can have a significant effect on OC cell viability. At 21 days, nearly complete cell death was achieved at a PTX concentration almost twice that of PTX-MPs in 3D cell models. The relatively large volume of Ca-Alg gel between the PTX-MPs and the 3D cellular construct served as an additional barrier to drug diffusion, as demonstrated in the release tests described above. This barrier likely delayed the cellular response and altered pharmacodynamics, particularly in comparison to conventional 2D and 3D cytotoxicity assays. On the other hand, these results highlight the potential of this 3D *in vitro* model for OC treatment, offering the advantage of prolonged PTX release compared to free PTX.

4. Conclusion

PLGA-MPs with an average diameter of 5 μm were prepared using a solvent evaporation technique, achieving a PTX loading around 5%. PLGA-MPs, both PTX-loaded and unloaded, were successfully encapsulated within Ca-Alg MBs (size 600–760 μm), obtained through a coaxial air jet bead generator.

In *in vitro* studies, PTX release from the MPs showed an initial burst for five days, followed by sustained release over two weeks, reaching 100% release by day 20. Encapsulation in alginate beads slowed the early release, likely due to the restriction of the gel matrix on PTX diffusion. Optical microscopy confirmed degradation of the encapsulated PLGA MPs, with near-total disappearance by day 21, coinciding with complete PTX release.

The biocompatibility and efficacy for this delivery system were tested in 2D SKOV-3 OC culture. PTX-MPs at concentrations up to 150 nM showed no cytotoxicity, while higher doses (450–1500 nM) significantly reduced viability within 7 days.

To better mimic *in vivo* conditions, a 3D bioprinted model of SKOV-3 cells was established to assess drug diffusion and cellular response over extended periods (up to 21 days). This model, maintained in culture for a longer time compared with the traditional 2D cell cultures, allowed for the evaluation of controlled drug release, cellular behavior, and chemical microenvironment features. The pharmacological effect of the PTX-MPs was evaluated in this 3D model over 21 days. PTX-MPs at 750 nM and 1500 nM efficiently killed SKOV-3 cells, with sustained viability reduction. Lower concentrations also showed continuous, slow cell death, highlighting the potential of PTX-MPs for controlled, persistent drug release.

In these 3D models, no toxicity from Alg-MBs was observed up to 21 days, even at high volumes. PTX-MBs delayed effects, showing no viability reduction at 72 h, but significant viability decreases at 7 days with higher concentrations (1500–3000 nM). At 21 days, nearly complete cell death occurred, highlighting the 3D model potential for prolonged PTX release in OC treatment.

This study highlights the effectiveness of a novel drug delivery system for sustained drug release and its potential application in OC therapies, where long-term localized treatment could significantly improve therapeutic outcomes.

Furthermore, the 3D culture system used in this study proved advantageous for testing this type of drug delivery systems, offering a more accurate representation of the *in vivo* tumor microenvironment, and providing a more reliable platform for assessing their pharmacological effects and their long-term impact on cancer cell viability.

CRediT authorship contribution statement

Cristina Chirizzi: Writing – review & editing, Methodology, Investigation. **Francesca Gorini:** Writing – review & editing, Methodology, Investigation. **Ilaria Porello:** Writing – review & editing, Methodology, Investigation. **Marco Malferrari:** Writing – review & editing, Methodology, Data curation. **Maila Becconi:** Investigation. **Elisa D'Arrigo:** Investigation. **Francesco Falciani:** Investigation. **Emma Coschina:** Investigation. **Stefania Rapino:** Writing – review & editing, Supervision, Methodology, Investigation, Conceptualization. **Anna Myriam Perrone:** Writing – review & editing, Supervision, Conceptualization. **Pierandrea De Iaco:** Writing – review & editing, Conceptualization. **Pierangelo Metrangolo:** Writing – review & editing, Conceptualization. **Francesca Baldelli Bombelli:** Writing – review & editing, Supervision, Methodology, Investigation, Data curation, Conceptualization. **Gloria Ravegnini:** Writing – review & editing, Supervision, Methodology, Investigation, Data curation, Conceptualization. **Francesco Cellesi:** Writing – review & editing, Writing – original draft, Supervision, Methodology, Investigation, Data curation, Conceptualization.

Funding

This work was supported by Regione Lombardia (POR FESR 2014 – 2020) within the framework of the NEWMED project (ID 1175999). E.C. acknowledges funding from the European Union – NextGenerationEU – through the Italian Ministry of University and Research (PNRR—M4C2-I1.3) Project PE_00000019 "HEAL ITALIA", CUP J33C22002920006.

Declaration of competing interest

The authors declare that they have no known competing financial interests or personal relationships that could have appeared to influence the work reported in this paper.

Acknowledgments

The authors deeply thank Simona Palange, Sara Colazzo, Marija Zovko, Laura Brambilla, Francesco Dimauro (Master students at the Department of Chemistry, Materials, and Chemical Engineerig "Giulio Natta", Politecnico di Milano, Italy) for their support with material preparation and characterization and Francesca Palla (student at the Department of Chemistry "Giacomo Ciamician", Bologna, Italy) for her support with 3D OC bioprinted constructs preparation.

Appendix A. Supplementary material

Supplementary data to this article can be found online at https://doi.org/10.1016/j.ijpharm.2025.125993.

Data availability

Data will be made available on request.

References

Armstrong, D.K., Fleming, G.F., Markman, M., Bailey, H.H., 2006. A phase I trial of intraperitoneal sustained-release paclitaxel microspheres (Paclimer) in recurrent ovarian cancer: a gynecologic oncology group study. Gynecol. Oncol. 103, 391–396.

Arokia Femina, T., Barghavi, V., Archana, K., Swethaa, N.G., Maddaly, R., 2023. Non-uniformity in in vitro drug-induced cytotoxicity as evidenced by differences in IC50 values – implications and way forward. J. Pharmacol. Toxicol. Methods 119, 107238.

Ashimova, A., Yegorov, S., Negmetzhanov, B., Hortelano, G., 2019. Cell encapsulation within alginate microcapsules: immunological challenges and outlook. Front. Bioeng. Biotechnol. 7.

Becconi, M., De Zio, S., Falciani, F., Santamaria, M., Malferrari, M., Rapino, S., 2023. Nano-electrochemical characterization of a 3D bioprinted cervical tumor model. Cancers.

Calafiore, R., Basta, G., 2014. Clinical application of microencapsulated islets: actual prospectives on progress and challenges. Adv. Drug Deliv. Rev. 67–68, 84–92.

Cantelli, A., Malferrari, M., Soldà, A., Simonetti, G., Forni, S., Toscanella, E., Mattioli, E. J., Zerbetto, F., Zanelli, A., Di Giosia, M., Zangoli, M., Barbarella, G., Rapino, S., Di Maria, F., Calvaresi, M., 2021. human serum albumin–oligothiophene bioconjugate: a phototheranostic platform for localized killing of cancer cells by precise light activation. JACS Au 1, 925–935.

Cellesi, F., Tirelli, N., Hubbell, J.A., 2004. Towards a fully-synthetic substitute of alginate: development of a new process using thermal gelation and chemical cross-linking. Biomaterials 25, 5115–5124.

Cymbaluk-Płoska, A., Sobolewski, P., Chudecka-Głaz, A., Wiśniewska, E., Łapczuk, J., Frankowski, M., Droździk, M., El Fray, M., 2019. Double-emulsion copolyester microcapsules for sustained intraperitoneal release of carboplatin. J. Function. Biomater. 10.

de Jesus, G.C., Gaspar Bastos, R., Altenhofen da Silva, M., 2019. Production and characterization of alginate beads for growth of immobilized Desmodesmus subspicatus and its potential to remove potassium, carbon and nitrogen from sugarcane vinasse. Biocatal. Agric. Biotechnol. 22, 101438.

Dwivedi, P., Han, S., Mangrio, F., Fan, R., Dwivedi, M., Zhu, Z., Huang, F., Wu, Q., Khatik, R., Cohn, D.E., Si, T., Hu, S., Sparreboom, A., Xu, R.X., 2019. Engineered multifunctional biodegradable hybrid microparticles for paclitaxel delivery in cancer therapy. Mater. Sci. Eng. C 102, 113–123.

Fagotti, A., Gallotta, V., Romano, F., Fanfani, F., Rossitto, C., Naldini, A., Vigliotta, M., Scambia, G., 2010. Peritoneal carcinosis of ovarian origin. World J. Gastrointest. Oncol. 2, 102–108.

Graham, R., MacDonald, N.D., Mould, T.A., Kotsopoulos, I.C., 2024. Hyperthermic intraperitoneal chemotherapy (HIPEC) in the management of ovarian cancer. Obstetr. Gynaecol. 26, 76–83.

Hariyadi, D.M., Islam, N., 2020. Current status of alginate in drug delivery. Adv. Pharmacol. Pharm. Sci. 2020, 8886095.

He, L., Shang, Z., Liu, H., Yuan, Z.X., 2020. Alginate-based platforms for cancer-targeted drug delivery. Biomed Res. Int. 2020, 1487259.

Kang, S.-M., Lee, G.-W., Huh, Y.S., 2019. Centrifugal force-driven modular micronozzle system: generation of engineered alginate microspheres. Sci. Rep. 9, 12776.

Kohane, D.S., Tse, J.Y., Yeo, Y., Padera, R., Shubina, M., Langer, R., 2006. Biodegradable polymeric microspheres and nanospheres for drug delivery in the peritoneum. J. Biomed. Mater. Res. A 77A, 351–361.

Larsson, P., Engqvist, H., Biermann, J., Werner Rönnerman, E., Forssell-Aronsson, E., Kovács, A., Karlsson, P., Helou, K., Parris, T.Z., 2020. Optimization of cell viability assays to improve replicability and reproducibility of cancer drug sensitivity screens. Sci. Rep. 10, 5798.

Leebmann, H., Piso, P., 2018. PIPAC and HIPEC-competing or supplementary therapeutic procedures for peritoneal metastases. Der Chirurg; Zeitschrift Fur Alle Gebiete Der Operativen Medizen 89, 693–698.

Liu, P., Krishnan, T.R., 1999. Alginate-pectin-poly-L-lysine particulate as a potential controlled release formulation. J. Pharm. Pharmacol. 51, 141–149.

Liu, Y., Ma, W., Zhou, P., Wen, Q., Wen, Q., Lu, Y., Zhao, L., Shi, H., Dai, J., Li, J., Fu, S., 2023. In situ administration of temperature-sensitive hydrogel composite loading paclitaxel microspheres and cisplatin for the treatment of melanoma. Biomed. Pharmacother. Biomed. Pharmacother. 160, 114380.

Lopez-Mendez, T.B., Santos-Vizcaino, E., Pedraz, J.L., Orive, G., Hernandez, R.M., 2021. Cell microencapsulation technologies for sustained drug delivery: latest advances in efficacy and biosafety. J. Control. Release 335, 619–636.

Muguruma, M., Teraoka, S., Miyahara, K., Ueda, A., Asaoka, M., Okazaki, M., Kawate, T., Kuroda, M., Miyagi, Y., Ishikawa, T., 2020. Differences in drug sensitivity between two-dimensional and three-dimensional culture systems in triple-negative breast cancer cell lines. Biochem. Biophys. Res. Commun. 533, 268–274.

Natsugoe, S., Tokuda, K., Shimada, M., Kumanohoso, T., Baba, M., Takao, S., Tabata, M., Nakamura, K., Yoshizawa, H., Aikou, T., 1999. Morphology of the designed biodegradable cisplatin microsphere. Anticancer Res 19, 5163–5167.

Neufeld, L., Yeini, E., Pozzi, S., Satchi-Fainaro, R., 2022. 3D bioprinted cancer models: from basic biology to drug development. Nat. Rev. Cancer 22, 679–692.

Pagnotta, G., Becconi, M., Malferrari, M., Aiello, D., Napoli, A., Di Lisa, L., Grilli, S., Rapino, S., Focarete, M.L., 2023. Development of a tissue construct with spatially controllable stiffness via a one-step 3D bioprinting and dual-crosslinking process. Mater. Adv. 4, 3491–3505.

Pannu, H.K., Bristow, R.E., Montz, F.J., Fishman, E.K., 2003. Multidetector CT of peritoneal carcinomatosis from ovarian cancer. Radiographics 23, 687–701.

Perelló-Trias, M.T., Serrano-Muñoz, A.J., Rodríguez-Fernández, A., Segura-Sampedro, J. J., Ramis, J.M., Monjo, M., 2024. Intraperitoneal drug delivery systems for peritoneal carcinomatosis: Bridging the gap between research and clinical implementation. J. Control. Release 373, 70–92.

Primavera, R., Bellotti, E., Di Mascolo, D., Di Francesco, M., Wang, J., Kevadiya, B.D., De Pascale, A., Thakor, A.S., Decuzzi, P., 2021. Insulin granule-loaded microplates for modulating blood glucose levels in type-1 diabetes. ACS Appl. Mater. Interfaces 13, 53618–53629.

Qi, M., Lacik, I., Kolláriková, G., Strand, B.L., Formo, K., Wang, Y., Marchese, E., Mendoza-Elias, J.E., Kinzer, K.P., Gatti, F., Paushter, D., Patel, S., Oberholzer, J., 2011. A recommended laparoscopic procedure for implantation of microcapsules in the peritoneal cavity of non-human primates. J. Surg. Res. 168, e117–e123.

Quail, D.F., Joyce, J.A., 2013. Microenvironmental regulation of tumor progression and metastasis. Nat. Med. 19, 1423–1437.

Rodrigues, J., Heinrich, M.A., Teixeira, L.M., Prakash, J., 2021. 3D In vitro model (R) evolution: unveiling tumor–stroma interactions. Trends Cancer 7, 249–264.

Sagiri, S.S., Pal, K., Basak, P., Rana, U.A., Shakir, I., Anis, A., 2014. Encapsulation of sorbitan ester-based organogels in alginate microparticles. AAPS PharmSciTech 15, 1197–1208.

Tempfer, C., Giger-Pabst, U., Hilal, Z., Dogan, A., Rezniczek, G.A., 2018. Pressurized intraperitoneal aerosol chemotherapy (PIPAC) for peritoneal carcinomatosis: systematic review of clinical and experimental evidence with special emphasis on ovarian cancer. Arch. Gynecol. Obstet. 298, 243–257.

Tsai, M., Lu, Z., Wang, J., Yeh, T.-K., Wientjes, M.G., Au, J.L.S., 2007. Effects of carrier on disposition and antitumor activity of intraperitoneal paclitaxel. Pharm. Res. 24, 1691–1701.

Tsai, M., Lu, Z., Wientjes, M.G., Au, J.L.S., 2013. Paclitaxel-loaded polymeric microparticles: quantitative relationships between in vitro drug release rate and in vivo pharmacodynamics. J. Control. Release 172, 737–744.

Win, S.Y., Chavalitsarot, M., Eawsakul, K., Ongtanasup, T., Nasongkla, N., 2024. Encapsulation of cyclosporine A-loaded PLGA nanospheres in alginate microbeads for anti-inflammatory application. ACS Omega 9, 6901–6911.

Wojtyła, C., Bertuccio, P., Giermaziak, W., Santucci, C., Odone, A., Ciebiera, M., Negri, E., Wojtyła, A., La Vecchia, C., 2023. European trends in ovarian cancer mortality, 1990–2020 and predictions to 2025. Eur. J. Cancer 194, 113350.

Wu, J., Kong, T., Yeung, K.W., Shum, H.C., Cheung, K.M., Wang, L., To, M.K., 2013. Fabrication and characterization of monodisperse PLGA-alginate core-shell microspheres with monodisperse size and homogeneous shells for controlled drug release. Acta Biomater. 9, 7410–7419.

Zhai, P., Chen, X.B., Schreyer, D.J., 2015. PLGA/alginate composite microspheres for hydrophilic protein delivery. Mater. Sci. Eng. C Mater. Biol. Appl. 56, 251–259.